scientific reports

Check for updates

OPEN

Radiomics-based machine learning model for diagnosing internal abdominal hernias: a retrospective study

Zhong-Kai Ni[1], Tian-Han Zhou[1], Shu-Chao Kang[2], Ye-Hong Han[1], Hai-Min Jin[1], Shi-Fei Huang[1] & Hai Huang[1]✉

Intraperitoneal hernia is an acute abdominal disease, with complex imaging features and variable clinical manifestations that challenge surgeons and emergency physicians in early disease assessment and streamlined diagnosis and treatment procedures. We retrospectively included patients with internal abdominal hernia between January 2021 and June 2024. Eight machine learning models were constructed, and the classifier with the best performance was selected based on comparative evaluation. The performance of each model was assessed using the area under the curve (AUC), accuracy, and specificity to determine the optimal radiomics-based predictive algorithm. A total of 107 radiomics features were extracted, revealing distinct features between herniated and normal intestines. A predictive model for internal abdominal hernias was constructed based on a machine learning algorithm incorporating 7 different features. The Random Forest model demonstrated superior performance, achieving an AUC of 1, accuracy of 90%, sensitivity of 80%, and specificity of 100% in validation set. Radiomics analysis of internal abdominal hernias provides substantial data support for early disease diagnosis, but it is still a need for validation with a larger sample size in the future.

Keywords Iinternal abdominal hernias, Radiomics, Small intestine necrosis, Machine learning

Internal abdominal hernia is a rapidly progressive condition and a significant contributor to the high mortality rate among patients with acute abdomen. Its diagnosis and management present substantial challenges for both surgeons and emergency physicians in clinical and surgical settings[1,2]. Due to the increasing prevalence of the non-operative management of internal hernias, methods such as spasmolysis, anti-inflammatory therapy, and interventional procedures are on the rise, complicating the early detection internal hernias[3]. Furthermore, elderly patients often present with nonspecific or atypical symptoms, resulting in delayed diagnosis and higher complication rates[4]. This condition is further complicated by the complex anatomy and mobility of the intestines, which often pose significant challenges for accurate imaging-based diagnosis. Radiomics is a computational approach that extracts high-dimensional quantitative features from medical images, to uncover patterns not discernible to the human eye. It has been successfully applied in oncology for tumor characterization, prognosis, and treatment response prediction[5,6].

In recent years, radiomics has shown promise in the evaluation of several acute abdominal conditions such as bowel ischemia and appendicitis[7]. However, its application in identifying internal abdominal hernias remains limited. The current literature lacks comprehensive studies that explore radiomic approaches specifically tailored for the early and accurate diagnosis of internal abdominal hernias[4].Our present study aims to investigate whether radiomic features extracted from CT imaging can effectively distinguish herniated intestines from normal structures in patients with acute abdomen. We hypothesize that internal abdominal hernias exhibit specific radiological patterns that can be quantitatively captured and modeled using radiomics, enabling earlier and more accurate diagnosis. By developing and validating a radiomic prediction model, we seek to enhance diagnostic precision and support clinical decision-making in this high-risk population.

[1]Department of General Surgery, Hangzhou Hospital of Traditional Chinese Medicine, No. 453 Ti-Yu-Chang Road, Hangzhou 310007, Zhejiang, People's Republic of China. [2]Department of Radiography, Hangzhou Hospital of Traditional Chinese Medicine, No. 453 Ti-Yu-Chang Road, Hangzhou 310007, Zhejiang, People's Republic of China. ✉email: nizhongkai@126.com

Methods

Patients

All patients who underwent surgery for suspected internal abdominal hernia between January 2021 and June 2024 were retrospectively screened. Inclusion criteria were: (1) diagnosis of internal abdominal hernia confirmed by abdominal CT; (2) surgical confirmation during intraoperative exploration; (3) availability of high-quality, preoperative abdominal enhanced CT scans. Patients were excluded if no internal hernia was identified during surgery or if imaging data were incomplete or of poor quality.Handling of patients with multiple surgeries: One patient who underwent two separate surgeries for recurrent internal abdominal hernia was included only once in the analysis to avoid duplication. For this patient, only the first CT scan and corresponding surgical findings were considered to maintain independence of observations. The study was approved by the ethics committee of Hangzhou Traditional Chinese Medicine Hospital of with the requirement for patient informed consent waived. All methods were performed in accordance with the relevant guidelines and regulations. The flowchart is illustrated in Fig. 1.

Equipment and segmentation

All CT examinations were performed using a Siemens Somatom dual-source scanner. Detailed scan parameters are provided in the supplementary materials1. To ensure image quality and minimize variability, all scans were acquired using a standardized protocol and were reviewed independently by two abdominal radiologists (each with over five years of experience) to assess for motion artifacts, noise, and resolution consistency. Only images free of significant artifacts and with sufficient contrast were included in the analysis. Radiomic analysis was

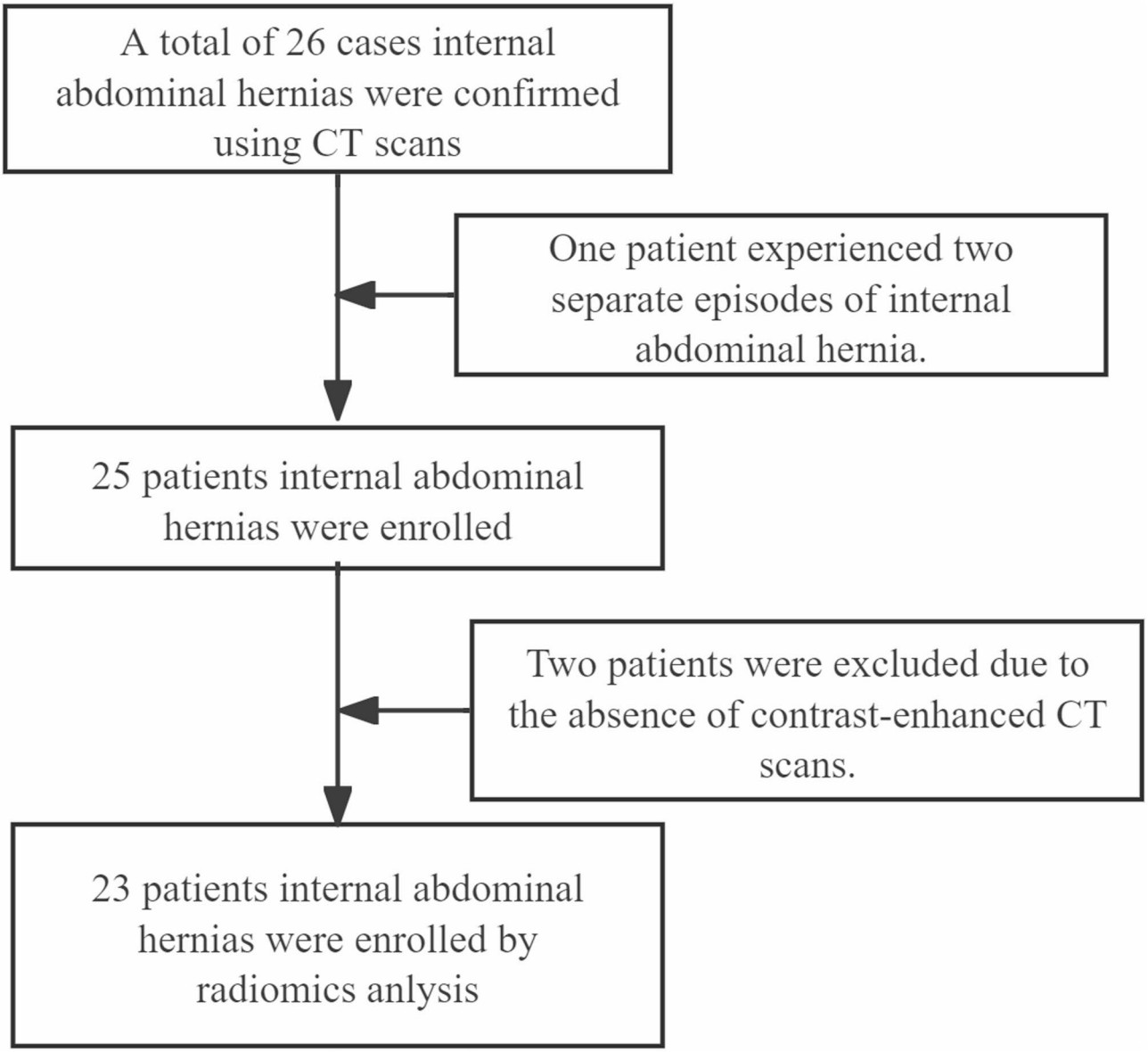

Fig. 1. The flowchart of this study.

performed using images from the arterial phase, which provides optimal delineation of bowel wall structures and is widely used in the evaluation of acute abdominal pathology. Images were stored in DICOM format, and regions of interest (ROIs) were manually delineated using ITK-SNAP (version 3.6.0). Representative CT images of internal abdominal hernias are presented in Fig. 2.

Feature extraction and selection

Features extraction involved first-order features, intensity histogram statistics, shape and size statistics, and texture features. These handcrafted features were extracted using an in-house feature analysis program implemented in PyRadiomics (http://pyradiomics.readthedocs.io). We have included a detailed list and description of all extracted features in the Supplementary Materials 2. First, highly redundant features were excluded by calculating the Spearman correlation coefficient, removing one of each pair that had a correlation coefficient > 0.8. Second, the Mann-Whitney U test was conducted to identify features that were significantly associated with treatment resistance, retaining those with a p-value < 0.05. The least absolute shrinkage and selection operator (LASSO) regression model was used on the training dataset for signature construction. Depending on the regulation weight *λ*, LASSO shrinks all regression coefficients towards zero and sets the coefficients of many irrelevant features precisely to zero. To find an optimal *λ*, 10-fold cross-validation with minimum criteria was employed, where the final value of *λ* yielded minimum cross-validation error. The retained features with nonzero coefficients were used for regression model fitting and combined into a radiomics signature.After Lasso feature screening, we performed supervised learning using eight different machine learning (ML) classifiers such as Random Forest (RF), k-nearest neighbor (KNN), logistic regression (LR), multilayer perceptron (MLP), and support vector machine (SVM), extreme gradient Boosting (XGBoost), and LightGBM, extra trees. We adopted five-fold cross-validation to obtain the final rad signature to determine the optimal classifier. The entire dataset was randomly partitioned into five subsets of approximately equal size. In each iteration, four subsets were used for training and one subset for validation. This process was repeated five times, such that each subset served once as the validation set. The final performance metrics were averaged across the five folds to ensure a robust and less prone to overfitting evaluation of the model.

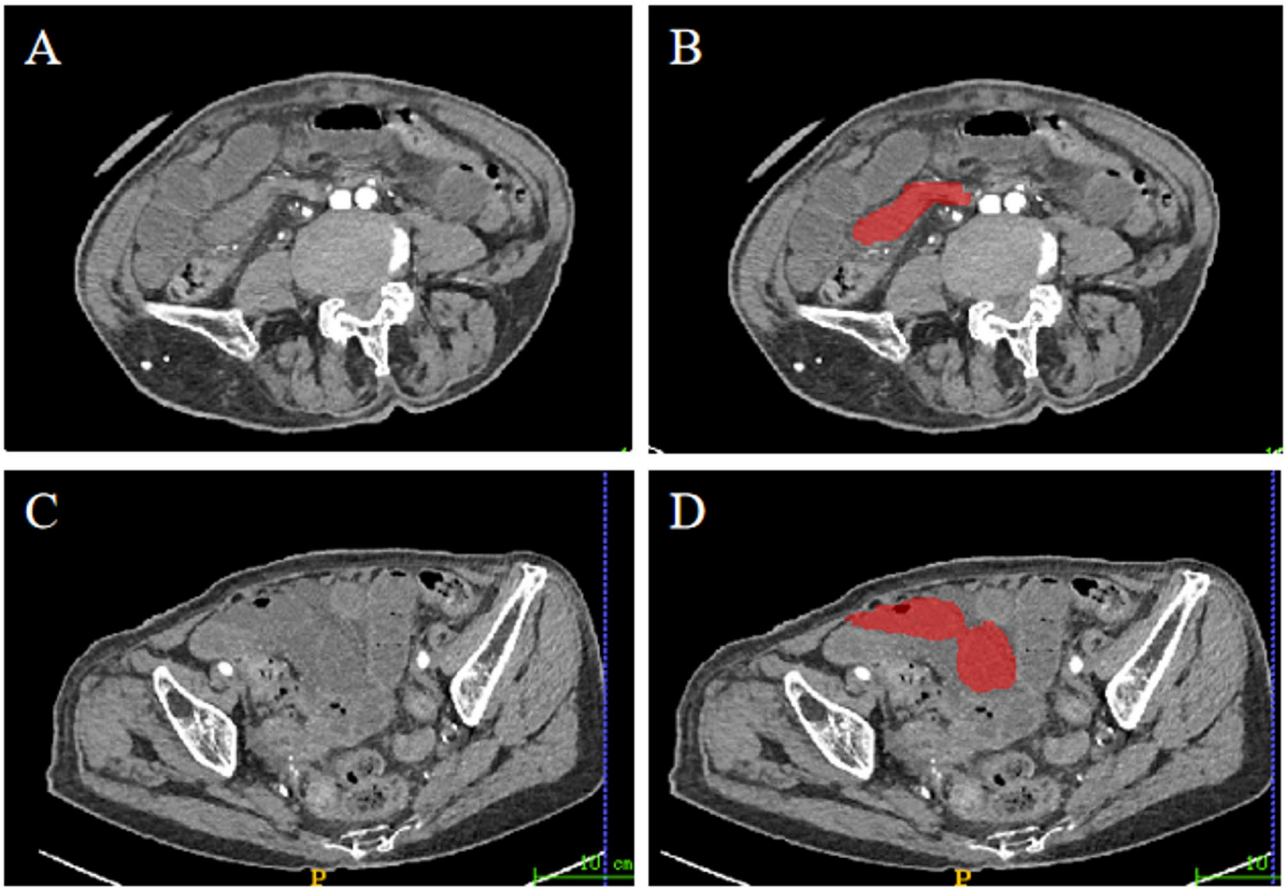

Fig. 2. ROI segmentation of small intestine and internal abdominal hernia in CT Cross-sectional. CT images of normal small intestine (**A**); the ROI of the normal small intestine (**B**); CT images of internal abdominal hernias (**C**); the ROI of the internal abdominal hernias (**D**).

Statistical analysis

In this study, descriptive statistics were used to describe the ultrasound imaging data and clinical data. Continuous variables were expressed as mean ± standard deviation (SD). Classification results obtained from each method were presented as absolute quantities and percentages. The accuracy (ACC), sensitivity (SEN), specificity (SPE), positive predictive value (PPV), negative predictive value (NPV), and F1 score for measuring the result consistency of all ML models to the gold standard were statistically assessed. Statistical tests for κ coefficient between different groups were performed. A p-value < 0.05 was considered statistically significant. SPSS 22 software was used for statistical data analysis.

Results

Demographics and characteristics

A total of 26 CT images were enrolled in our study. The included patients comprised 15 male patients and 10 female patients, ranging in age from 31 to 90 years, with an average age of 62 ± 16.73 years. The baseline of patients and the causes of internal abdominal hernia are shown in Table 1. One patient developed an adhesive band post-reduction, resulting in a new internal hernia and requiring subsequent surgery at another hospital. Two patients were excluded due to the absence of contrast-enhanced CT imaging. Our analysis focused on the high-throughput data from these 23 CT images.

Radiomics features selection and signature building

We extracted radiomics features for normal intestinal segments without hernia and pathological segments affected by internal abdominal hernia from 23 CT images. Internal abdominal hernias were confirmed in all patients through laparoscopy or open surgery, and no postoperative pathological evidence of abdominal tumors was found in patients undergoing small intestine resection. We extracted a total of 107 radiomics features (supplementary materials 2), and their distributions are shown in Fig. 3. After analysis, satisfactory reproducibility of radiomics feature extraction was achieved. The LASSO algorithm was employed in the

ID	Gender	Age	Time of onset (hour)	The duration of conservative treatment (hour)	Enhanced CT examination	Surgical duration (min)	Intestinal necrosis	Postoperative exhaust time (hour)	History of abdominal surgery	The causes of intra-abdominal hernia
1	Female	31	24	3	Yes	64	No	18	Cesarean section (2020)	Hiatus of broad ligament of uterus
2	Female	81	6	0	Yes	115	Yes	66	Hysterectomy (1994)	fibrous bands
3	Female	80	8	1	Yes	140	Yes	90	None	Annular defect of the greater omentum
4	Male	68	6	0	Yes	79	No	67	Radical gastrectomy (2023)	Fibrous bands
5	Male	63	24	3	Yes	150	Yes	90	None	Fibrous bands
6	Male	57	47	7	Yes	63	No	36	None	fibrous bands
7	Female	89	70	2	Yes	135	Yes	118	None	Fibrous bands
8	Female	90	5	2	Yes	138	Yes	77	None	Fibrous bands
9	Male	68	23	2	No	118	No	93	Gastric perforation, subtotal gastrectomy(2024)	Fibrous bands
10	Male	39	46	2	Yes	135	No	107	Appendectomy(The exact time is unknown)	fibrous bands
11	Female	53	11	2	Yes	120	No	16	Hysterectomy (2021)	Fibrous bands
12	Male	66	2	39	Yes	57	No	50	None	Fibrous bands
13	Female	49	12	2	Yes	90	No	18	None	Fibrous bands
14	Male	75	6	5	Yes	100	No	68	Radical gastrectomy (2021)	The mesenteric hiatus is not closed
15	Male	68	67	8	Yes	55	No	43	None	Fibrous bands
16	Female	43	45	70	Yes	145	Yes	46	Cesarean Sect. (2004)	Hiatus of broad ligament of uterus
17	Male	64	21	83	Yes	135	No	121	None	Fibrous bands
18	Female	57	2	23	Yes	55	No	14	None	Abnormal development of the treitz ligament
19	Male	35	12	1	Yes	213	Yes	87	Appendectomy (The exact time is unknown)	Fibrous bands
20	Male	65	10	40	Yes	170	No	96	None	Fibrous bands
21	Female	86	23	115	Yes	101	Yes	163	None	Fibrous bands
22	Male	35	10	4	No	153	No	28	None	Fibrous bands
23	Male	66	15	7	Yes	75	No	142	None	Fibrous bands
24	Male	63	2	2	Yes	60	No	112	Radical gastrectomy (The exact time is unknown)	Fibrous bands
25	Male	59	20	3	Yes	60	No	68	None	The intestines intertwine with each other

Table 1. Basic patient data and surgical information.

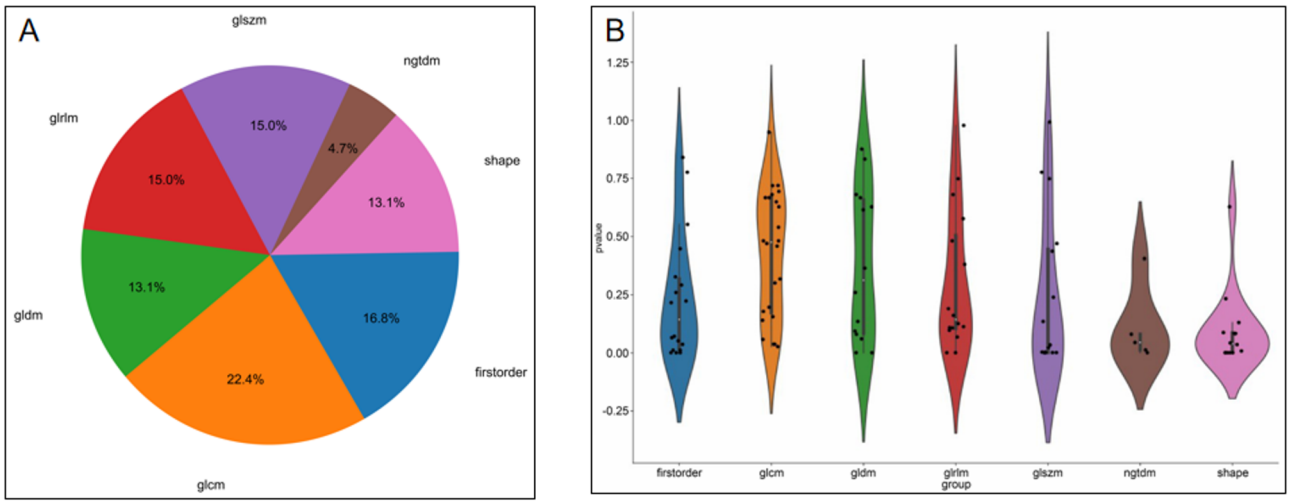

Fig. 3. Distribution of (**A**) radiomics features and (**B**) features statistical test.

training cohort to determine the optimal regulation weight (λ = 0.0518), and 7 radiomics features were chosen for distinguishing between normal bowel and bowel affected by internal abdominal hernia (Fig. 4).

Establishment of the ML-assisted visual approaches and radiomics

Eight classical machine learning models were selected to work as the base models in this study. We then performed supervised learning using different machine learning classifiers. The optimal model was obtained using radiomics features compared with an LR, SVM, KNN, MLP, RandomForest, ExtraTrees, XGBoost, and LightGBM classifier. Figure 5 shows the accuracy of each radiomics signature model on the training cohort and test cohort. Compared to the other seven ML classifiers, the RF model achieved the best AUC value in the test cohort, reaching 0.909 in distinguishing between normal bowel and bowel affected by internal abdominal hernia. The accuracy, sensitivity, specificity of the RF model was 90%, 80.%, 100% in the test cohort (Table 2). The probability distribution demonstrates the diagnostic performance of the model during external validation, indicating that the RF model did not encounter any diagnostic errors in the test cohort.

Discussion

Cause analysis of internal abdominal hernia

Internal abdominal hernia is categorized according to the cause as either congenital internal abdominal hernia or acquired internal abdominal hernia, caused by surgery, trauma, inflammation, and other factors that can result in defects in the greater omentum or lesser omentum[8]. We reviewed the causes of Internal abdominal hernia in Tabel 1. Interestingly, only seven out of 19 patients with hernia rings formed by abdominal fiber bands had a history of abdominal surgery. Studies indicate that with increasing age, the abdominal cavity may be affected by inflammation, spontaneous proliferation, and abnormal differentiation, leading to the formation of fibrous bands[9]. However, in imaging analysis, the fiber band ring is often difficult to distinguish from the surrounding tissue using the naked eye. In postoperative patients, incomplete closure of the mesangial hiatus and inadequate adherence of the omentum to form adhesive bands are often considered as initial factors contributing to postoperative internal abdominal hernias[10]. Congenital defects and structural abnormalities within the abdominal cavity also require some attention[11]. This is thought to be a feature that can appear significantly different from that of normal tissue based on radiomics studies.

Early clinical manifestations of internal hernia and correction of internal environment disorder

Intestinal obstruction often manifests as the initial symptom of an internal abdominal hernia, which was particularly noteworthy in patients without a history of abdominal surgery[12]. In cases where intestinal obstruction occurs for the first time, there is the significant likelihood of an internal abdominal hernia, with rapid progression requiring special attention. Early detection is crucial for preventing intestinal ischemia, which can progress to peritonitis or aggravated abdominal distension, potentially leading to necrotic exudation of the intestines[13]. Decreased intestinal wall density and abnormal blood supply vessels on enhanced CT are important ischemic features. Rapidly sounding the alarm in such cases is a critical focus of this study. When homeostasis of the internal environment is disrupted, prompt fluid replacement is generally necessary[14]. Pre-intervention to maintain water-electrolyte and acid-base balance before they become disrupted is essential for safe surgery and postoperative rehabilitation. The uniform decrease in the density of the edematous intestine may also lead to bias in later radiomics studies[15]. In our study, we also recorded the duration of conservative treatment prior to surgery. We observed that, over time, bowel edema evolves and may lead to progressive changes in imaging features. This highlights the potential value of developing time series–based radiomics models in future studies to capture dynamic imaging changes and improve diagnostic accuracy in patients undergoing delayed intervention[16].

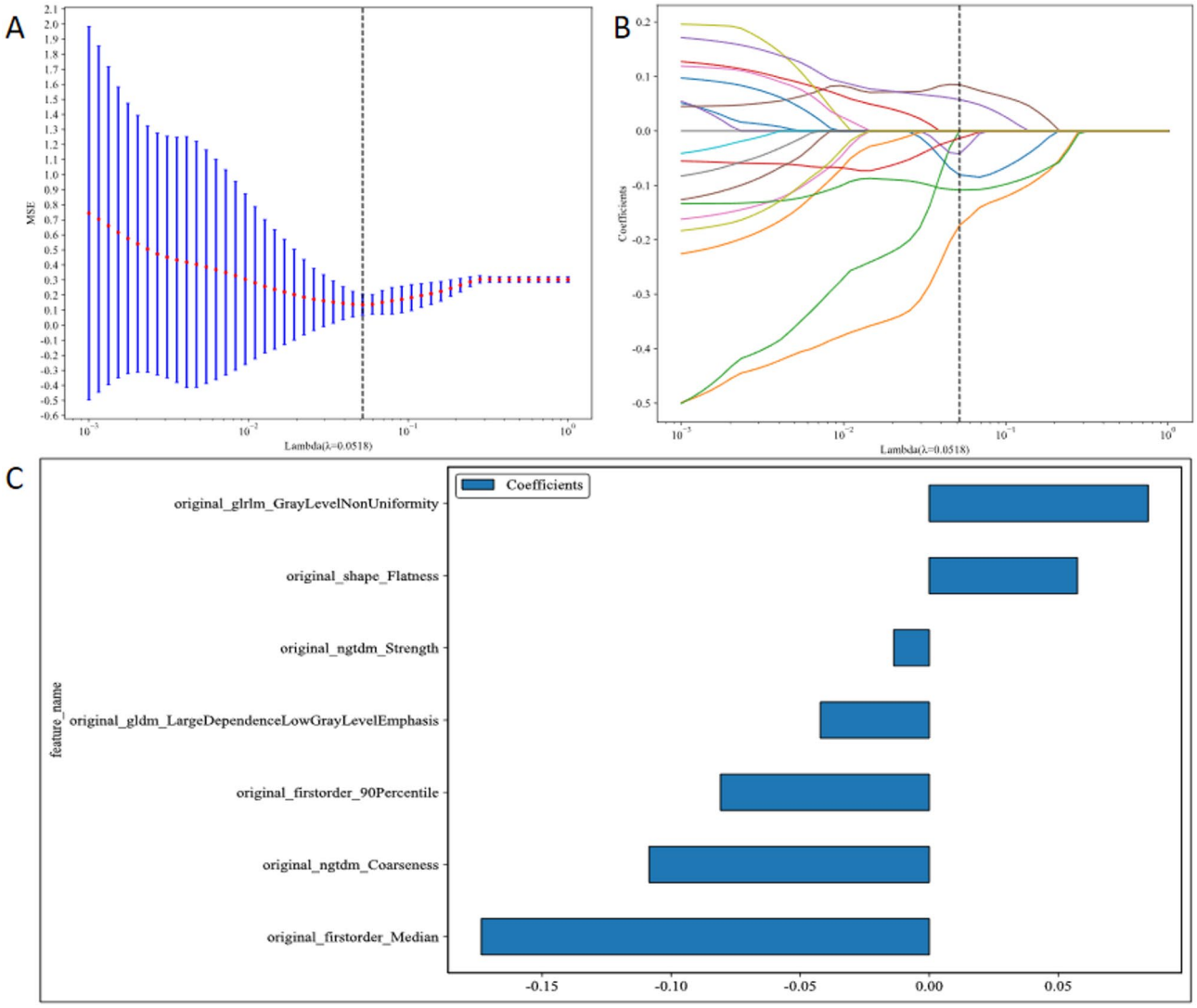

Fig. 4. (**A**) Regularization effect plot; (**B**) Lasso path diagram; (**C**) 19 radiomics features after lasso selection.

Early identification and radiomics study

Early intervention for internal hernias is of great value, as these conditions are often difficult to recognize clinically. Imaging examinations play a crucial role in their diagnosis. According to Mathieu, typical radiographic features on barium studies include encapsulated clusters of dilated bowel loops in abnormal positions, crowding or stacking of small bowel within a hernia sac, and signs of obstruction such as segmental dilatation and delayed transit. On CT, further diagnostic clues may be observed, such as mesenteric vascular abnormalities—manifesting as congestion, crowding, twisting, and stretching of the mesenteric vessels—which are valuable indicators of potential internal herniation[2]. Internal hernias can manifest indirectly on CT images with signs like spiral patterns, segmental intestinal dilation, intestinal wall ischemia, and beak amputation of the bowel[4]. Ederveen also investigated the use of CT for predicting internal hernias in patients following Roux-en-Y surgery with a diagnostic accuracy of 83.8%, a specificity of 87.1%, a positive predictive value of 53.4%, and a negative predictive value of 96.8%[17]. We identified seven radiomic features that effectively distinguish normal bowel from internal herniation. Affected bowel segments may exhibit small bowel dilatation, restricted passage of contrast agents, increased intraluminal contents, and bowel wall edema with exudative changes. These pathophysiological alterations may underlie the observed differences in radiomic features.

Intraoperative decisions regarding bowel condition and surgical resection

Our findings support the potential of radiomic analysis as a valuable decision-support tool for the early detection of internal abdominal hernias and timely surgical management.While clinicians repeatedly review patient images and analyze image data, preoperative preparation should also be encouraged. We advocate shifting from a mindset of diagnosis followed by treatment to one that constantly prepares for imminent surgical intervention[18]. Five patients in this study were > 80 years old, and the final surgery confirmed strangulated intestinal necrosis in all of them. Given the rapid progression of abdominal and systemic infections in such cases,

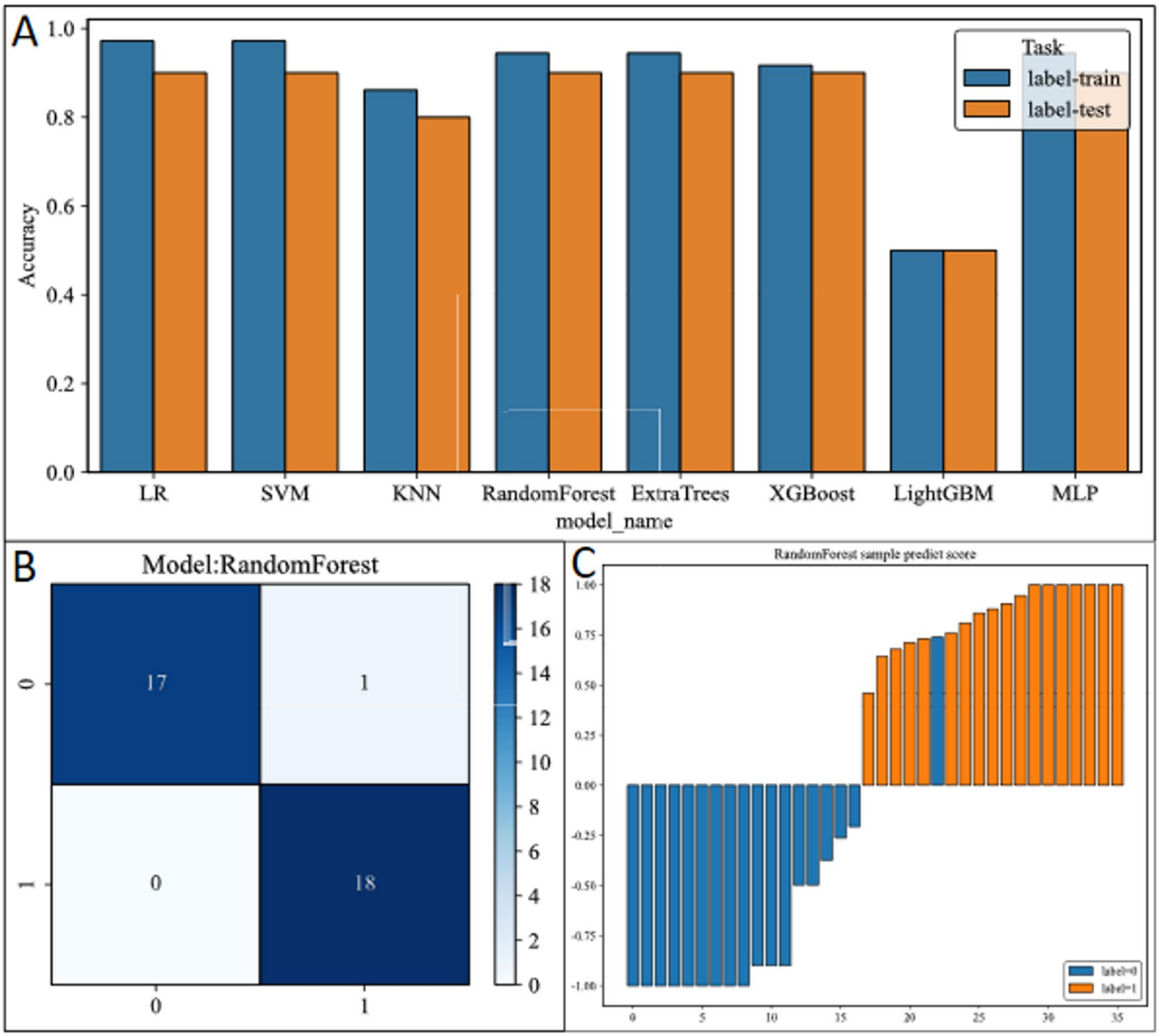

Fig. 5. (**A**) Accuracy of seven machine learning models in the training set and the validation set; (**B**) confusion matrix in the validation set; (**C**) RandomForest sample predict score in validation dataset.

systematic and meticulous preoperative assessment should be replaced by a critical assessment approach[19]. Once it is confirmed that there are no life-threatening organ failures or significant contraindications to surgery, the surgical procedure should proceed swiftly. The time of incarceration, size of the hernia ring, degree of mesangial edema and rotation, and state of mesangial arteriosclerosis can significantly affect the blood supply to the entire small intestine when entrapped by the hernia ring[20]. We developed a diagnostic model based on CT images capable of rapidly flagging potential internal hernia cases. This model holds promise for early identification and triage of suspected internal hernias in clinical settings, thereby facilitating timely surgical consultation and aiding decisions regarding emergency surgical intervention.

Limitations

Firstly, the sample size is limited, which affects the generalizability of the model's findings and increases the risk of overfitting. To reduce the risk of overfitting due to small sample size, we used multi-step feature selection, 5-fold cross-validation, and excluded models with significant overfitting. Future research should aim to utilize larger sample sizes for comprehensive radiomics and big data analysis to better predict intestinal vitality preoperatively and guide surgical decisions and methods and postoperative assessment. Then, the complexity of manual outlining and the intricacies of intestinal structures may impact the reproducibility of the research. All CT images were reviewed and manually segmented by two board-certified abdominal radiologists. Discrepancies in ROI annotations were resolved by consensus to reduce inter-observer variability and ensure consistent labeling for feature extraction. At the same time, identifying time-dependent radiological features

Model_name	Accuracy	AUC	95% CI	Sensitivity	Specificity	PPV	NPV	Task
LR	0.972	1.000	1.000–1.000	0.944	1.000	1.000	0.947	train
LR	0.900	1.000	1.000–1.000	0.800	1.000	1.000	0.833	test
SVM	0.972	1.000	1.000–1.000	0.944	1.000	1.000	0.947	train
SVM	0.900	1.000	1.000–1.000	0.800	1.000	1.000	0.833	test
KNN	0.861	0.965	0.916–1.000	0.833	0.889	0.882	0.842	train
KNN	0.800	0.940	0.799–1.000	0.800	0.800	0.800	0.800	test
RandomForest	0.944	0.985	0.952–1.000	0.944	0.944	0.944	0.944	train
RandomForest	0.900	1.000	1.000–1.000	0.800	1.000	1.000	0.833	test
ExtraTrees	0.944	0.997	0.988–1.000	0.889	1.000	1.000	0.900	train
ExtraTrees	0.900	1.000	1.000–1.000	0.800	1.000	1.000	0.833	test
XGBoost	0.917	0.998	0.994–1.000	0.833	1.000	1.000	0.857	train
XGBoost	0.900	1.000	1.000–1.000	0.800	1.000	1.000	0.833	test
LightGBM	0.500	0.500	1.000–1.000	0.000	1.000	0.000	0.500	train
LightGBM	0.500	0.500	1.000–1.000	0.000	1.000	0.000	0.500	test
MLP	0.944	0.988	0.961–1.000	0.889	1.000	1.000	0.900	train
MLP	0.900	1.000	1.000–1.000	0.800	1.000	1.000	0.833	test

Table 2. Predictive model based on machine learning algorithms.

associated with intestinal viability plays an important role in guiding surgical decision-making and represents a promising direction for future research.

Conclusions

This study demonstrates the potential of CT radiomics analysis in assisting the early diagnosis of internal abdominal hernias. Such an approach may facilitate the rapid identification and triage of suspected cases, enabling timely surgical consultation and informed decision-making. In addition, future research is warranted to explore spatiotemporal radiomic features that may help assess bowel viability, which is critical for optimizing surgical strategies.

Data availability

Data is provided within the manuscript or supplementary information files.

Received: 21 December 2024; Accepted: 14 May 2025
Published online: 22 May 2025

References

1. Surel, A. A., Işık, N. İ. & Yazla, M. Untangling diagnostic confusion in internal abdominal hernias. *Turk. J. Trauma Emerg. Surg.* **29**, 1114–1121 (2023).
2. Selçuk, D., Kantarci, F., Oğüt, G. & Korman, U. Radiological evaluation of internal abdominal hernias. *Turk. J. Gastroenterol.* **16**(2), 57–64 (2005).
3. Yang, T. W. W. et al. Non-operative management for small bowel obstruction in a Virgin abdomen: A systematic review. *ANZ J. Surg.* **91**(5), 802–809 (2021).
4. Blachar, A., Federle, M. P. & Dodson, S. F. Internal hernia: Clinical and imaging findings in 17 patients with emphasis on CT criteria. *Radiology* **218**(1), 68–74 (2001).
5. Zhou, T. et al. Comparative analysis of machine learning-based ultrasound radiomics in predicting malignancy of partially cystic thyroid nodules. *Endocrine* **83**, 118–126 (2024).
6. Ni, Z. et al. Radiomics and deep learning for large volume lymph node metastasis in papillary thyroid carcinoma. *Gland Surg.* **13**(9), 1639–1649 (2024).
7. Liang, D. et al. Development and validation of a deep learning and radiomics combined model for differentiating complicated from uncomplicated acute appendicitis. *Acad. Radiol.* **31**(4), 1344–1354 (2024).
8. Berle, M., Dahlslett, K. H., Kavaliauskiene, G. & Hoem, D. Internal abdominal hernia. *Tidsskr Nor Laegeforen* **137**(16) (2017).
9. Podda, M., Khan, M. & Di Saverio, S. Adhesive small bowel obstruction and the six W's: Who, how, why, when, what, and where to diagnose and operate? *Scand. J. Surg.* **110**, 159–169 (2021).
10. Ende, V., Devas, N., Zhang, X., Yang, J. & Pryor, A. D. Internal hernia trends following gastric bypass surgery. *Surg. Endosc.* **37**, 7183–7191 (2023).
11. Sajan, A. et al. Herniation through defects in the broad ligament. *JSLS* **25**, e2020 (2021).
12. Yamada, M. et al. Small bowel obstruction due to internal hernia caused by the vermiform appendix, mesentery of the small intestines, and greater omentum in a patient with no history of abdominal surgery. *Gan Kagaku Ryoho* **49**, 1556–1558 (2022).
13. Dou, L., Yang, H., Wang, C., Tang, H. & Li, D. Adhesive and non-adhesive internal hernia: clinical relevance and multi-detector CT images. *Sci. Rep.* **9**, 12847 (2019).
14. Cihoric, M. et al. Inflammatory response, fluid balance and outcome in emergency high-risk abdominal surgery. *Acta Anaesthesiol. Scand.* **65**, 730–739 (2021).
15. Okino, Y. et al. Root of the small-bowel mesentery: Correlative anatomy and CT features of pathologic conditions. *Radiographics* **21**(6), 1475–1490 (2001).
16. Pszczolkowski, S. et al. Quantitative CT radiomics-based models for prediction of haematoma expansion and poor functional outcome in primary intracerebral haemorrhage. *Eur. Radiol.* **31**(10), 7945–7959 (2021).

17. Ederveen, J. C., van Berckel, M. M. G., Nienhuijs, S. W., Weber, R. J. P. & Nederend, J. Predictive value of abdominal CT in evaluating internal herniation after bariatric laparoscopic Roux-en-Y gastric bypass. *Br. J. Surg.* **105**(12), 1623–1629 (2018).
18. Taghavifar, S. et al. Computed tomography in emergency diagnosis and management considerations of small bowel obstruction for surgical vs. non-surgical approach. *Curr. Med. Imaging* **18**, 275–284 (2022).
19. Ruiz, M. et al. Physical and cognitive function assessment to predict postoperative outcomes of abdominal surgery. *J. Surg. Res.* **267**, 495–505 (2021).
20. Kakisako, J. et al. Quadruple (1440 degrees) intestinal volvulus. *Clin. Case Rep.* **12**, e9022 (2024).

Author contributions

Z.-K.N. and T.-H.Z. contributed equally to this work. Z.-K.N. (Master Candidate) is in charge of conceiving and designing the study and writing the manuscript. T.-H.Z. (Master Candidate) is in charge of providing critical revisions that are important for the intellectual content. S.-C.K. (Master Candidate) is in charge of is in charge of image data quality control and reconstruction analysis.Y.-H.H. (Master Candidate) , H.-M.J. (Master Candidate) and S.-F.H. (Master Candidate) are in charge of collecting the data and analyzing and interpreting the data. H.H. (Doctoral Candidate) is in charge of approving the final version of the manuscript.

Funding

For this study, Zhejiang Traditional Medicine and Technology Program China (Grant NO. 2022ZA119) and Zhejiang Province science and technology plan projects (2025KY1163)provided financial support. The authors have no other conflicts of interest to declare.

Declarations

Competing interests

The authors declare no competing interests.

Additional information

Supplementary Information The online version contains supplementary material available at https://doi.org/10.1038/s41598-025-02534-6.

Correspondence and requests for materials should be addressed to H.H.